Solution Chemical Synthesis of nanostructured Thermoelectric Materials

Xiaohua Ji,*[a] Terry M. Tritt,[a] Xinbing Zhao[b] and Joe. W. Kolis[c]

[a] *118 Kinard Laboratory, Department of Physics & Astronomy, Clemson University, Clemson, SC 29634, USA. Fax:1 864 656 0805; Tel: 1 864 656 4594; E-mail: xiaohji@clemson.edu*
[b] *Department of Materials Science & Engineering, Zhejiang University, Hangzhou 310027, Zhejiang,P. R. China. Tel:+86 571 87951451; E-mail: zhaoxb@zju.edu.cn*
[c] *Department of Chemistry, Clemson University, Clemson, SC 29634, USA. E-mail: kjoseph@clemson.edu*

Received June 18, 2008

The ability to mass produce thermoelectric nano-powders is crucial to the thermoelectric nano and nano-composite research. Solution chemical synthesis, such as hydrothermal, solvothermal and low temperature solution chemical syntheses are effectual approaches to manufacture nano materials with acceptable yield. By carefully designing the reaction agents and controlling the synthesis parameters, numerous nanoscale materials with various morphologies could be achieved. In this paper, the synthesis of nanosized state-of-the-art thermoelectric materials, such as Bi_2Te_3, $CoSb_3$, PbTe & PbSe, Bi_2S_3 etc. were presented, their multiple morphologies were displayed, and the underlying reaction mechanisms were discussed. Our lately developed hydrothermal nano-plating technique was also briefly introduced.

1. Introduction

The performance of a thermoelectric (TE) material is evaluated by its figure of merit $Z = \alpha^2/\rho\kappa$, where α is the Seebeck coefficient, ρ is the electrical resistivity, and κ is the thermal conductivity, which includes the contributions from both carriers and phonons, i.e. $\kappa = \kappa_e + \kappa_l$. A nanostructure, as indicated by its prefix, has one of its crucial dimensions on the order of 1-100 nm. In recent years, low dimensional or nanostructured thermoelectric materials has become an active research field of TE study, mostly motivated by the presence of increased electron density of states at the Fermi level in nanostructured materials and the possibility of exploiting boundary scattering to reduce the thermal conductivity[1]. Theoretical calculations of low dimensional TE materials have predicted a significant enhancement in *ZT* as the film thickness in two dimensional (2D) systems[2] or the wire diameter in one-dimensional (1D) systems[3] is decreased, benefiting from both quantum confinement effects to carriers and pronounced phonon scattering at the boundaries. Besides low-dimensional thin films or nanowire arrays, which might be mainly used in a micro-electro-mechanical system (MEMS), bulk TE materials are of more interest for their broad applications in commercial Peltier modules and power generation devices. The decision to pursue the concept of bulk nanocomposite thermoelectrics comes primarily from the heat transport management point of view as a way to further improve the figure of merit of the existing materials, as the bulk nanocomposite approach has the advantage of working in a dual manner[4]. Moving to lower dimensions could improve the electronic properties via quantum effects, notably the Seebeck coefficient, while introducing nanoparticles should lower the lattice thermal conductivity by effectively reducing the phonon mean free path. Using modern rapid sintering techniques such as spark plasma sintering (SPS), it is possible to form nanostructured bulk materials from nanopowders without significant grain growth by reducing both time and temperature needed for the densification. However, to make bulk nanocomposite, a practical question would be how to grow various thermoelectric nano powders with an acceptable yield?

A variety of techniques are available to produce nanostructured powders. Means like rapid solidification[5], atomization[6] and high energy ball milling[7] could be categorized as physical techniques. Other than these physical techniques, chemical approaches, such as Chemical Vapor Deposition (CVD), reduction & co-deposition, sol-gel, and so on, are all effectual nano preparation routes. Among which, hydrothermal / solvothermal synthesis, are attracting more and more attentions on the synthesis of nanostructured powders due to their advantages of low cost, very high yield, low energy consumption, short duration and most important, versatility, which will be demonstrated in this paper.

Hydrothermal synthesis is one of the important methods for producing fine powder of oxides. A hydrothermal system is usually maintained at a temperature beyond 100 ^oC and the autogenous pressure of water exceeds the ambient pressure, which is favorable for the crystallization of products. Research indicates that the hydrothermal method is also a practical means for preparing chalcogenide and phosphide nano materials. Similar to hydrothermal synthesis, in a solvothermal process[8], a non-aqueous solvent, which is sealed in an autoclave and maintained in its superheated state, is the reaction medium, where the reactants and products are prevented effectively from oxidation and volatilization and the reaction and crystallization can be realized simultaneously. Furthermore, organic solvents may be favorable for the dispersion of non-oxide nano-crystallites and may stabilize some metastable phases. Hydrothermal and solvothermal syntheses are both commonly used methods to prepare nanostructured powders with controllable size and morphology these days.

Concerning our own work, we've been applying solution chemical methods, including hydrothermal and solvothermal approaches to prepare nano thermoelectric materials for several years. By utilizing and continuously developing these techniques, various nanoscale state-of-the-art thermoelectric compounds,

such as Bi_2Te_3, $CoSb_3$, PbTe & PbSe, Bi_2S_3, Bi-Sb-Te & Bi-Te-Se, etc., with multiple nanostructures, have been successfully synthesized. In this paper, some of these synthesizing works, along with our lately developed hydrothermal nano-plating technique, will be presented.

2. Solution chemical synthesis of Bi_2Te_3 nanostructures

Bismuth telluride, Bi_2Te_3, and its alloys are most important semiconductor thermoelectric materials used in state-of-the-art thermoelectric devices for the 200 – 400 K temperature range. The figure of merit, *ZT* of the best bulk Bi_2Te_3 based alloys is about unit. It was reported that the figure of merit of Bi_2Te_3 based materials were significantly improved by making them into quantum dot superlattices[9] and nanowires[10].

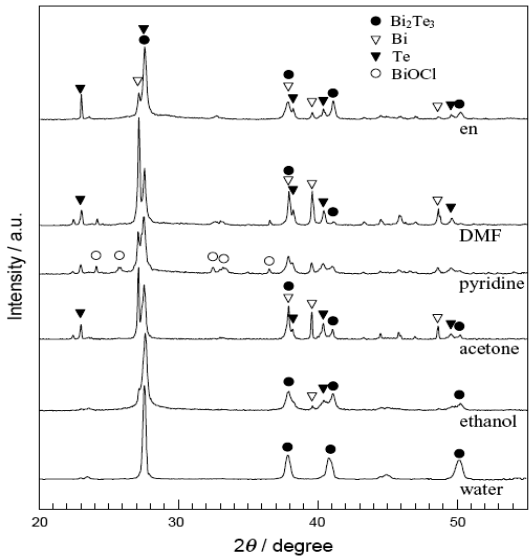

Fig.1 The XRD patterns of the solvothermally synthesized Bi_2Te_3 with different solvents as reaction medium (From the top to bottom: en, DMF, pyridine, acetone, ethanol and distilled water).

The solution chemical syntheses of nanosturctured Bi_2Te_3 were extensively studied by us in recent years. According to the standard reduction potentials, i.e. $E^0_{Bi^{3+}/Bi} = 0.200V$, $E^0_{Te^{4+}/Te} = 0.568V$, $E^0_{Te/Te^{2-}} = -1.143V$ and $E^0_{H_2O/BH_4^-} = -1.24V$, $BiCl_3$, Te powders, Na_2TeO_3 or TeO_2 were mainly selected as precursor-compounds and $NaBH_4$ as reductant. To anchor a best solvent for the Bi_2Te_3 synthesis, ethylenediamine (en), N,N-Dimethylformamide (DMF), pyridine, acetone, ethanol or distilled water were employed as reaction medium, respectively[11]. The XRD results in Fig.1 indicated that only when distilled water was employed as solvent could the final product achieve pure Bi_2Te_3 phase with $R\bar{3}m$ rhombohedral lattice structure. So thereafter we would utilize distilled water as solvent unless otherwise noted.

Our experiment[12] also indicated that both hydrothermal (sealed system, above 100 °C) and low-temperature aqueous solution synthesis (opened system, below 100 °C) work well on the preparation of nano Bi_2Te_3, and different Te sources such as Te powder, Na_2TeO_3 and TeO_2 are equally effective on leading to pure phase Bi_2Te_3. The XRD patterns of the as-prepared samples are shown in Fig.2, which suggested a single-phase-nature for all the final products. However, it is also revealed that under the same conditions, the samples synthesized at higher temperature & sealed system (H1, H2 and H3) carried better crystallinity than the samples synthesized at lower temperature & opened system (L1, L2 and L3), while the samples synthesized using Te powder (L3 and H3) also bear out better crystallinity than the other samples that using Na_2TeO_3 (L1 and H1) and TeO_2 (L2 and H2) as Te source.

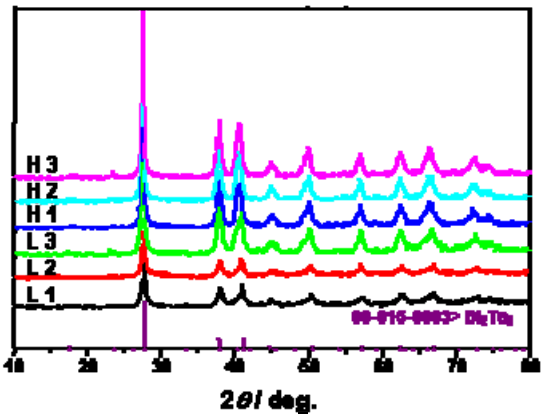

Fig.2 The XRD patterns of hydrothermally (L1, 2 and 3) and low temperature aqueously (H1,2 and 3) synthesized Bi_2Te_3 with different Te sources.

Ligands with poly-functional group, such as ethylenediaminetetraacetic acid disodium (EDTA) and Cetyl trimethylammonium bromide (CTAB), etc., can be used as structure directing agents to control the morphology of nanoparticles, mostly because these "soft-templates" tend to coordinate with several inorganic ions to form multinuclear complexes. For instance, as displayed in Fig.3, Bi_2Te_3 flowerlike and featherlike nanostructures, as well as Bi_2Te_3 hexagonal-chips and Bi_2Te_3 nanorods have been achieved via an EDTA-assisted hydrothermal process at 150 °C[13].

Based on our observations and analysis, possible reaction mechanisms involved in the hydrothermal synthesis of Bi_2Te_3 may be described as follows:

$$BiCl_3 + H_2O \rightarrow BiOCl + 2HCl \quad (1)$$

$$2BH_4^- + 2Bi^{3+} + 6OH^- \rightarrow 2H_2BO_3^- + 2Bi + 5H_2\uparrow \quad (2)$$

$$3Te + 6OH^- \rightarrow 2Te^{2-} + TeO_3^{2-} + 3H_2O \quad (3)$$

$$TeO_3^{2-} + BH_4^- \rightarrow Te_{a+1}^{2-} + H_2BO_3^- + H_2\uparrow \quad (4)$$

$$Te_{a+1}^{2-} \rightarrow a:Te + Te^{2-} \quad (5)$$

Here Te_{a+1}^{2-} is an amorphous poly-telluride colloid. Compared with the original solid tellurium powder, the poly-telluride colloid can be regarded as an active Te source. Reaction formula (4) also serves the turn when using Te compounds such as Na_2TeO_3 and TeO_2 as instead of Te powder as Te source.

In the final stage, the formation of the Bi_2Te_3 could be a combination of two independent pathways, that is, an ionic reaction process and an atomic reaction process. On one hand, the Bi^{3+} would react with the Te^{2-}; On the other hand, a directly

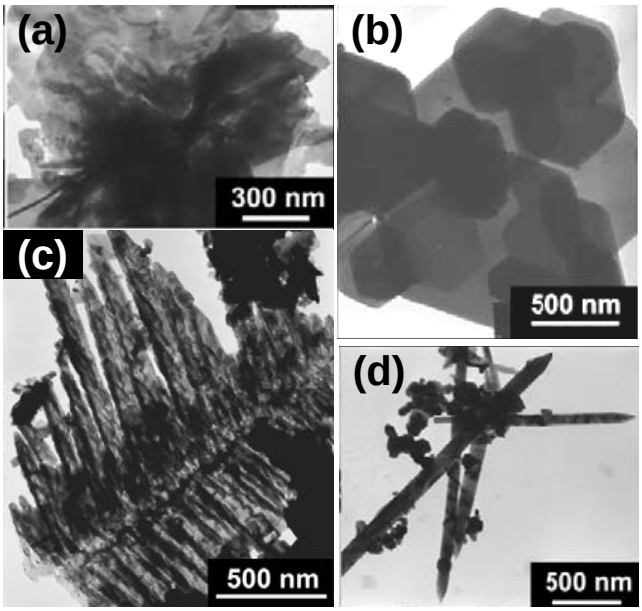

Fig. 3 Various Bi_2Te_3 nanostructures have been achieved via an EDTA-assisted hydrothermal synthesis: (a) flowerlike structure, (b) hexagonal chips, (c) featherlike structure and (d) Bi_2Te_3 nanorods.

atomic reaction process could parallelly proceed between the elemental Bi reduced from Bi^{3+} by $NaBH_4$ and poly-telluride colloid:

$$2Bi + 3(a{:}Te) \rightarrow Bi_2Te_3 \quad (6)$$

$$2Bi^{3+} + 3Te^{2-} \rightarrow Bi_2Te_3 \quad (7)$$

Novel fullerene-related structures like nanotubes would be of interest to improve the TE properties of bismuth telluride based materials, since nanotubes possess both low-dimensional and hollow structure features, and could be hopeful "phonon-glass electron-crystal" (PGEC) thermoelectric materials[14,15]. Since the first report on WS_2 nanotubes by Tenne and co-workers in 1992[16], nanotubes of various metal chalcogenides have been synthesized, such as $MoSe_2$, WSe_2 [17], ZrS_2 and HfS_2[18] of AB_2-type compounds, and CdSe, CdS[19] and NiS[20] of AB-type compounds. Being similar to these compounds, A_2B_3-type thermoelectric chalcogenides, such as Bi_2Te_3, Bi_2Se_3, and Sb_2Te_3, also carry trigonal and quasi-layered lattice features with van-der-Waals bonding between neighbouring chalcogen atomic layers. This makes it possible for them to form hollow cylindrical structures.

Nanotubes of A_2B_3-type chalcogenides were first synthesized by us via hydrothermal approach. Two hydrothermal routes for the synthesis of TE Bi_2Te_3 nanotubes, a higher temperature high pressure (HTHP) route in a sealed autoclave at 150 °C or above and a lower temperature normal pressure (LTNP) route in a beaker at 60 ~80°C were used therein[21].

Fig.4 (a) shows a cluster of Bi_2Te_3 nanotubes synthesized by the HTHP route. The as-synthesized nanotubes are 30 – 100 nm in diameters and up to 1 μm or longer in lengths. The inset in Fig.4 (a) shows three parallelly arranged nanotubes with closed ends. The electron diffraction (ED) pattern indicates that the tubes are of single crystalline. From the HRTEM image of a Bi_2Te_3 nanotube, Fig.4 (b), the thickness of the tube wall can be estimated as ~ 20 nm. The wall is not smooth but uneven and spiral instead. The enlarged picture of a smaller nanotube in Fig.4 (b) reveals the typical structure of a tube wall. One may see that the *c*-axis of the Bi_2Te_3 rhombohedral lattice is at an angle of about 30° to the normal direction of the wall. The tilted atomic planes form a spiral wall like a continuously developed pencil-shaving.

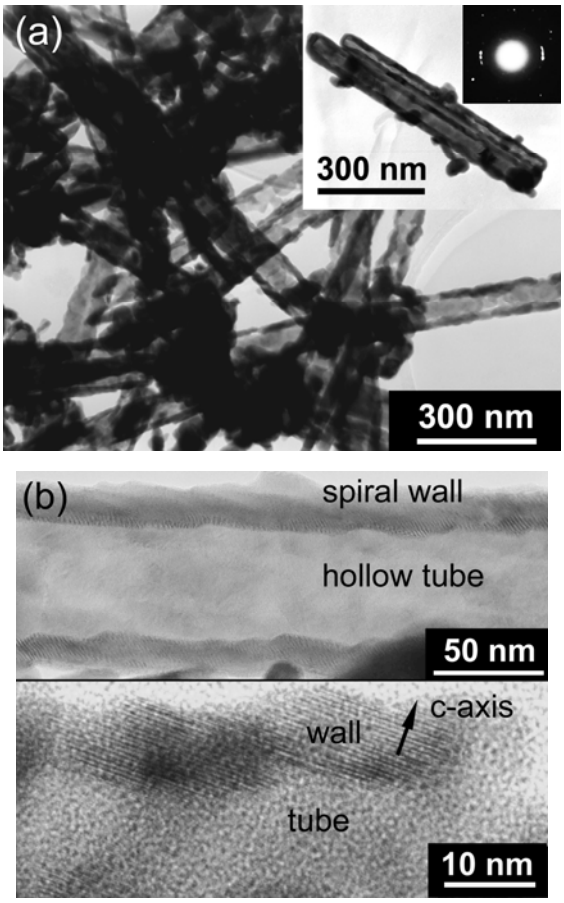

Fig.4 TEM (a) and HRTEM images (b) of the Bi_2Te_3 nanotubes hydrothermally synthesized in a sealed autoclave at 150°C.

The LTNP route is similar to the HTHP one but conducted in an open system at a lower temperature under ambient pressure. As shown in Fig.5, the as-prepared sample has a novel morphology of bubble-like short nanotubes, which we called "nanocapsules". The sizes of the nanocapsules measured from Fig.5 (a) are about 100 – 200 nm in diameters and 300–1500 nm in lengths. The wall thickness estimated from Fig.5 (b) is about 6 nm, which corresponds to double of the lattice parameter of the Bi_2Te3 *c*-axis of $c = 3.044$ nm according to JCPDS 82-0358. The TEM image shows also that most of the capsules have closed ends. Open ends, however, can also be found in Fig.5 (a). We also observed that the capsules are often forked as they have several branches. In the enlarged TEM photo of a branched nanocapsule, Fig.5 (b), one can see the angle between two branches is about 120°, corresponding to the hexagonal lattice structure of Bi_2Te_3. There are also small curved sheets in the powder, which could be a fragment falling from a broken

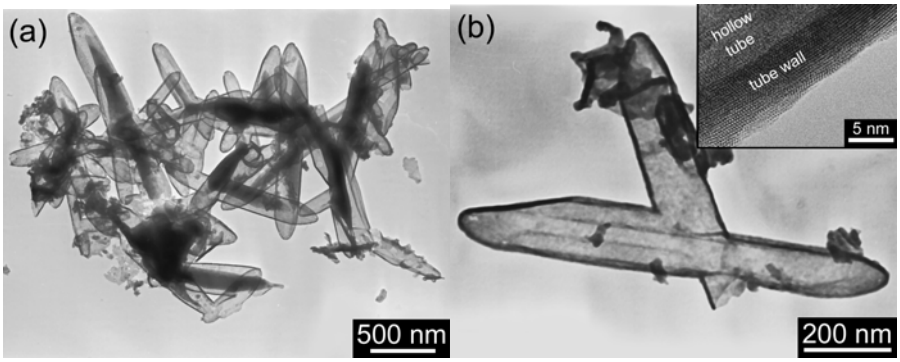

Fig. 5 TEM images of Bi_2Te_3 nanocapsule clusters (a) and a branched nanocapsule (b) hydrothermally synthesized in an open system at 65°C. The inset in (b) is a HRTEM image of the nanocapsule.

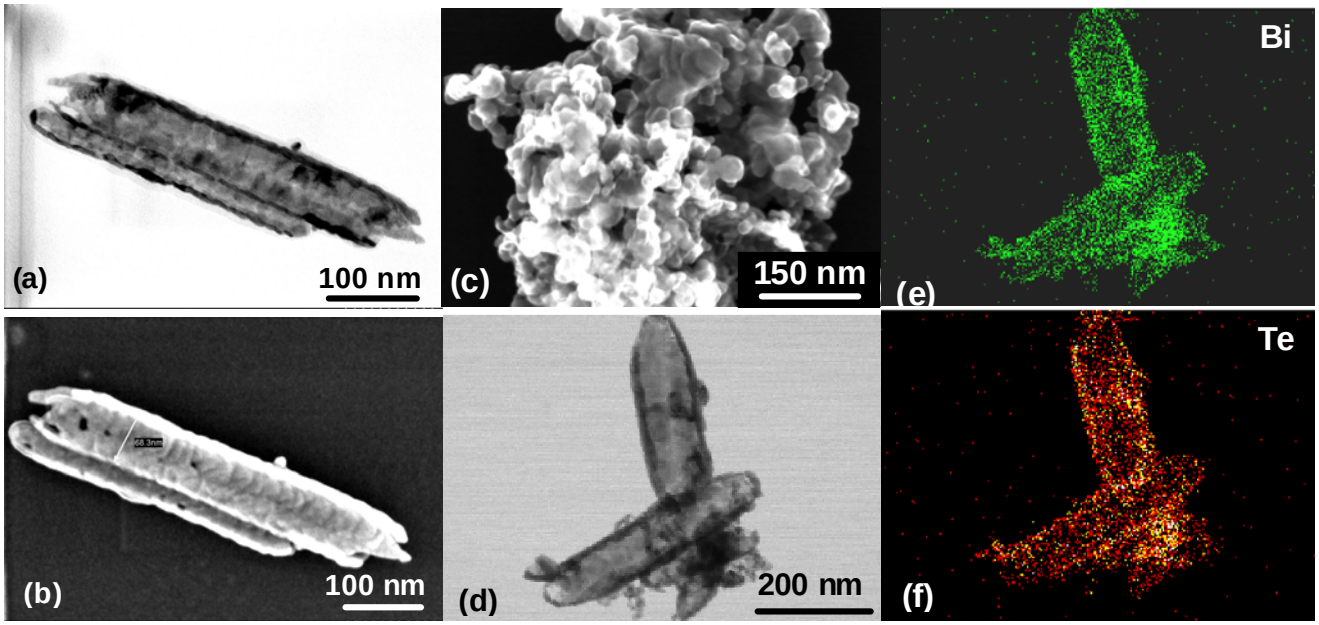

Fig.6 TEM image of two parallelly arranged Bi_2Te_3 nanotubes (a) with the corresponding SEM image (b); ~25 nm uniform Bi_2Te_3 spherical granules (c); A mapping EDS analysis on a two overlapped nanotubes reveals the nanotubes contain both Bi (e) and Te (f) elements.

nanocapsule but might also be an unclosed developing capsule or a tube nucleus.

Some more Bi_2Te_3 nanotubes, spherical granules and a mapping Energy Dispersive Spectrum (EDS) of two overlapped nanotubes are shown in Fig.6.

3. Solvothermal synthesis of $CoSb_3$ nanoparticles

Skutterudites are strongly covalently bonded compounds. Interests in these materials were greatly increased by the introduction of the phonon "glass electron crystal (PGEC)" concept[22]. $CoSb_3$ is one of the most commonly studied skutterudites, it has a cobalt cubic structure with antimony rings occupying six of the cells and two remaining empty[23]. Skutterudites are known for their high electron mobilities and favorable Seebeck coefficients. Unfortunately, the binary skutterudites also have large values of lattice thermal conductivity. Solutions to this obstacle have been attempted by filling the voids in the skutterudite lattice with elements that are loosely bound and are able to ''rattle'', thus, providing an extra phonon-scattering mechanism[24,25].

$CoSb_3$ were traditionally prepared by solid state reaction. To decrease the lattice thermal conductivity without fill it with "rattler", we proposed to make nano $CoSb_3$ via solvothermal approach. $CoCl_2$ and $SbCl_3$ were chosen as precursor-compounds, and absolute ethanol was designed as solvent, an appropriate amount of $NaBH_4$ was also introduced into reaction system as reductant. Our experimental indicated that $NaBH_4$ played a key role on the development of cobalt antimonide, most likely because of its energy supply and strong reduction effect. Without the attendance of $NaBH_4$, cobalt antimonide wouldn't come into being. The products' phase transited from Sb_2Co to $CoSb_3$ with the $NaBH_4$ dosage increase, as the XRD patterns shown in Fig.7 revealed. One possible explanation is that $CoSb_3$ could only be formed when the system energy reached to a certain threshold. Limited by the upper temperature limit of Teflon liner, the

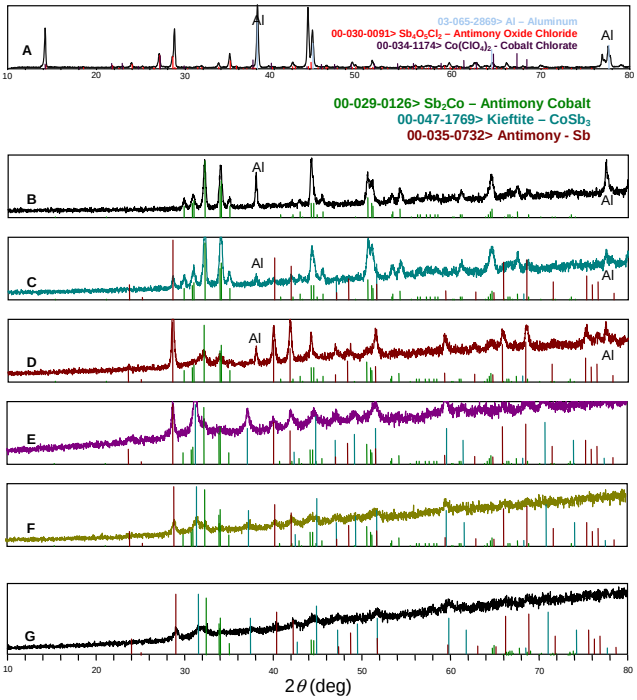

Fig.7 XRD patterns of powders solvothermally synthesized with different $NaBH_4$ dosage (From Sample A~G, corresponding to 0 g , 0.1 g, 0.2 g, 0.4 g, 0.8 g, 1 g and 1.6 g respectively).

synthesis time and temperature contributed little to the product phase in present work.

We found that single-phased $CoSb_3$ was difficult to be obtained directly from the present solvothermal syntheses, residual elemental Sb and a small amount of Sb_2Co were always observed in the synthesized products. Comparing the standard redox potentials (E^{θ}/V) of Co and Sb: $Co^{2+}/Co = -0.28$ V, while $Sb^{3+}/Sb = 0.204$ V, it is apparent that Sb^{3+} ions are much easier to be reduced by BH_4^- to Sb atoms than Co^{2+} to Co:

$$3SbCl_3 + 9NaBH_4 = 3Sb + 9BH_3 + 9NaCl + 9/2H_2\uparrow \quad (8)$$

And this reaction could be relatively fast, so at the beginning of synthesis, Co^{2+} ions abounded in the solution. The elemental Sb is stable once they precipitated, while the excess Co^{2+} ions were still dissolved in the solution. The chemical reaction in this solvothermal process is speculated complicated.

An acid wash was applied and finally single-phased $CoSb_3$ skutterudites were achieved. The as-prepared $CoSb_3$ powders composed of fine granular particles with very narrow size distribution of 15 - 20 nm, as shown in Fig. 8. Fig.9, a mapping EDS further proved the as-prepared $CoSb_3$ nanoparticles contain Co and Sb elements, and both elements distributed evenly on the matrix.

4. Solvothermal synthesis of PbTe & PbSe nanostructures

Lead chalcogenides PbX (X–Te, Se, S) are narrow band-gap semiconductors, which are widely used as sensors for infrared radiation, thermoelectric devices, photoresistors, lasers and other

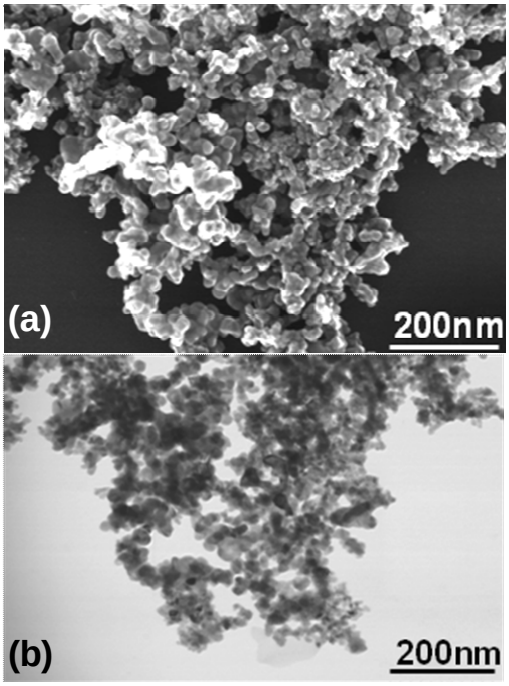

Fig. 8 The SEM image (a) and corresponding TEM image (b) of the solvothermally prepared $CoSb_3$ nano spheres.

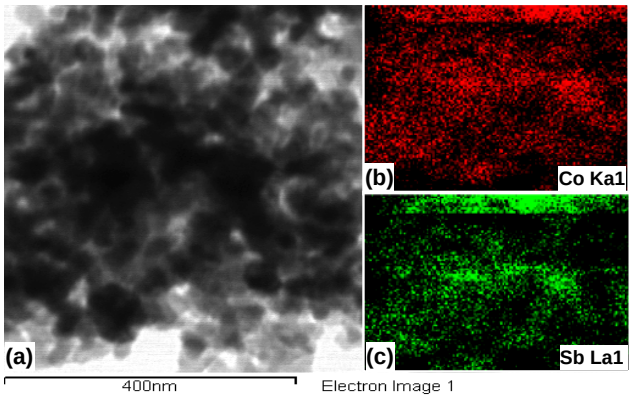

Fig. 9 A mapping EDS analysis of as-prepared $CoSb_3$ nano powders.

electronic devices[26]. The narrow and direct band gap natures make PbTe and PbSe one of the most important thermoelectric materials applied at medium temperature regime. It has been extensively reported that the thermoelectric or photovoltaic performances lead chalcogenides could be significantly improved by making them nanostructured. From the aspect of thermoelectrics, the nanostructure of PbTe or PbSe may potentially lower the thermal conductivity and improve the Seebeck coefficient as well.

In a typical solvothermal synthesis PbTe or PbSe, stoichiometry amount of $PbCl_2$ and Te (Se) powders (–325 mesh) were mixed together into a beaker. Ethylenediamine (en) were used as reaction solvent since Pb is apt to be oxidized. A small portion of en that could fully swamp the chemicals was poured into the beaker. The beaker was sitten into an ultrasonic cleaner to promote the dissolution of the chemicals. The mixture was then transferred into the autoclave. Followed by the remained en

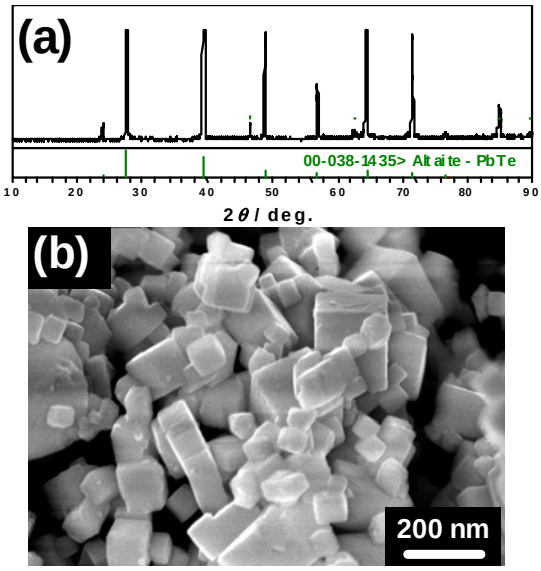

Fig. 10 XRD pattern of solvothermally synthesized PbTe, which agrees well with PDF 038-1435 cubic PbTe (a) and its dominate morphology of ~80 nm nano cubes (b).

added, the autoclave was sealed, maintained at 120 - 180 ^{o}C for 10 - 24 hrs.

Our nearly 20 growths indicated that among these syntheses, only when the temperature reaches 180 ^{o}C or higher could the pure phased PbTe (PbSe) be achieved (Fig.10 (a)). When the reactions were carried out below 180 ^{o}C, some amount of the elemental tellurium became residual, most likely due to the incomplete reaction. Moreover, the addition of $NaBH_4$ would lead to residua of elemental Pb in the final products. Considering the standard reduction potentials $E^{0}_{Pb^{2+}/Pb} =$ - 0.54V, $E^{0}_{Te/Te^{2-}} =$ - 1.143V, the major reaction in the solution should be ionic, i.e.:

$$Pb^{2+} + Te^{2-}_{a+1} \rightarrow PbTe + (a{:}Te) \quad (9)$$

And the reaction mechanism of PbSe is similar.

In our work, due to the rock-salt like lattice feature of PbTe, cubic PbTe nano-particles with average dimension of ~80 nm are the dominant morphology, as shown in Fig.10 (b).

For PbSe, surfactant Sodium dodecyl sulfate (SDS) was added into the solution during synthesis, as a result, some special morphology showed up in the final products. For example, gift-box-like cubic micro-sized structures and flower-like nanostructures came out, as shown in Fig.11 (a) and (b), respectively. It is also of interest that the diverse functions of the surfactant have been embodied on these two morphologies: the formation of the "gift-wrap" may attribute to the self-assembly role of SDS, while the flower-like structures are mainly due to the different interaction between surfactant and different facets of the cubic particles[27].

5. Hydrothermal synthesis of Bi_2S_3 nanostructures

Bismuth sulfide (Bi_2S_3) is a nearly direct band-gap semiconductor with layered orthorhombic lattice structure. The band gap of bulk Bi_2S_3 is about 1.3 eV. Bismuth sulfide has numerous potential applications in the fields of thermoelectrics

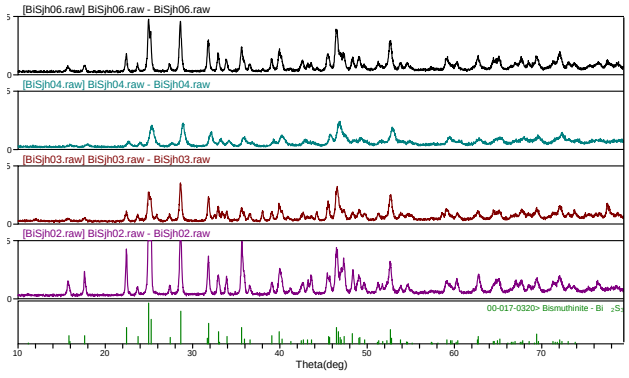

Fig.12 The XRD patterns of the hydrothermally synthesized Bi_2S_3

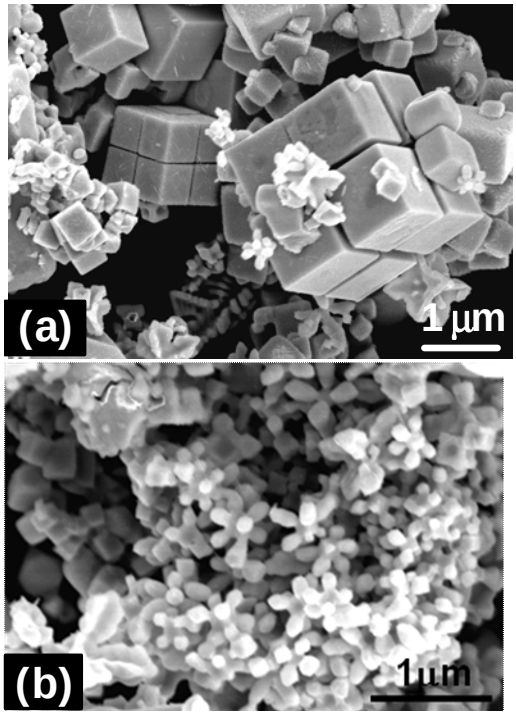

Fig. 11 The nanostructures of PbSe obtained via a SDS-assisted solvothermal synthesis.

(V-VI semiconductor, same type with the benchmark thermoelectric material Bi_2Te_3)and photodiode arrays and photovoltaics (due to the possibility of tuning different sizes of sub components). It has also been proposed as a good electrode of liquid-junction of solar cells.

In our work, $BiCl_3$ was chiefly selected as Bi source and Na_2S or S powder as S sources. Thioglycolic acid (TGA) is the organic compound $HSCH_2COOH$, which is an extensively used complexing ligand due to its containing of -SH radicle, so does Mercaptosuccinic acid (MSA). Besides the complexing function, TGA and MSA may also serve as S sources. The combination of $BiCl_3$ + MSA, $BiCl_3$ + Na_2S, $BiCl_3$ + Na_2S + TGA and $BiCl_3$ + S powder + TGA were applied as precursors, and distilled water as reaction medium in our experimental. The autoclaves were heated up to 180 ^{o}C, maintained for 48 hrs for reactions, then

cooled down to 50 ^{o}C and kept for another 48 hrs for the chelating taking effect.

As the XRD patterns shown in Fig.12, all samples exhibited pure Bi_2S_3, which agreed well with PDF-017-0320 orthorhombic Pbnm lattice structure. Among them, the XRD pattern of top 2nd sample ($BiCl_3$ + Na_2S + TGA) displayed the biggest half width.

Our experience indicated that the nano Bi_2S_3 prepared by solution chemical synthesis is apt to form 1-D structure. All our hydrothermally prepared Bi_2S_3 took on a basic shape of nanorod, whereas multiple morphologies derived from it, for example, nanorods with different aspect ratios, nano-bundles, flower-like nanostructures and ultra long nanowires, as exhibited in Fig.13.

Some more relevant investigations are shown in Fig.14. Fig.14 (a) and (b) are TEM images of some very uniform and regular Bi_2S_3 nanorods with dimensions of ~20 nm in diameters and lengths of up to several micros. The high-resolution TEM (HRTEM) image in Fig.14 (c) clearly suggested its layered lattice structure and the growth direction of the nanorods are along [2 -1 0]. The peaks in the Raman spectrums of 4 samples (Fig.14 (e))

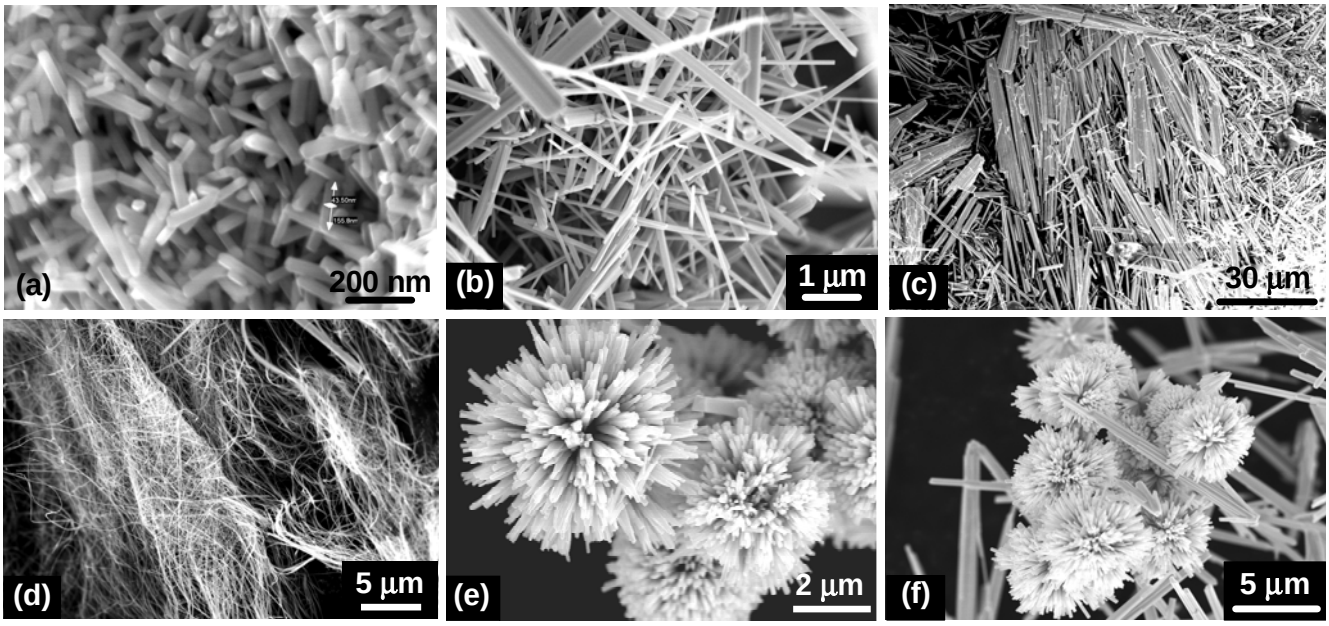

Fig. 13 Various morphologies of the hydrothermal synthesized Bi_2S_3 nanostructures, including short nanorods (a), long nanorods (b), nanobundles (c), mesh-like ultra-long nanowires with the aspect ratio of up to 5000 (d) and flower-like nanostructures (e) and (f), which are also consisted of Bi_2S_3 nanorods.

agree well with the theoretical values of 238 and 259 cm^{-1} [28]. The absorbance peaks in photoluminescence (PL) spectrum (Fig.14
(d)) of 2 nano Bi_2S_3 samples showed remarkable blue-shifts, while the band gaps changed from 1.30 eV of the bulk- Bi_2S_3 to 1.42 and 1.45 eV, individually. These blue shifts could be attributed to the large aspect ratios and the quantum confinement effects of the current Bi_2S_3 nanorods and nanowires.

6. Solvothermal/hydrothermal nano-plating technique

As an extension of the current solvothermal / hydrothermal synthesis technique, instead of mechanically mixing the bulk grains with nano particles to fabricate nano-composite thermoelectrics, we also proposed the solvothermal/hydrothermal nano-plating technique. The basic idea is to put the micro-sized TE bulk grains into the solvothermal / hydrothermal environment and allow the nano-particles grow directly onto the surface of the bulk-matrix grains. Upon the subsequent densification, the nano-particles would remain on the grain boundaries and a more homogeneous bulk-nano-composite would be achieved.

As a proof-of-principle study, $CoSb_3$ bulk-nano-composite was fabricated by this technique and the results are quite satisfied[29]. In this work, we present three samples: a bulk sample to serve as a reference and two samples with solvothermally plating nanostructures of 5 wt% and 20 wt%, respectively. All three samples used the same bulk starting materials. After the solvothermal nano-plating, the bulk grain was covered with a fluffy layer that made up of a mass of nano-particles (Fig. 15 a-c). The nanoparticle layers remained and in turn became part of the grain boundary upon the consequent hot pressing, and relatively homogeneous nanocomposites are thus achieved, as clearly seen in Fig. 15 d-f. The thermal conductivity was measured via two independent techniques (steady state and laser flash) and both show a systematic reduction in the thermal conductivity with an increasing amount of nanostructures.

This solvothermal/hydrothermal nano-plating technique was thereafter applied on many other materials system, such as Bi_2Te_3 and PbTe, homogeneously or heterogeneously, all showed promising results.

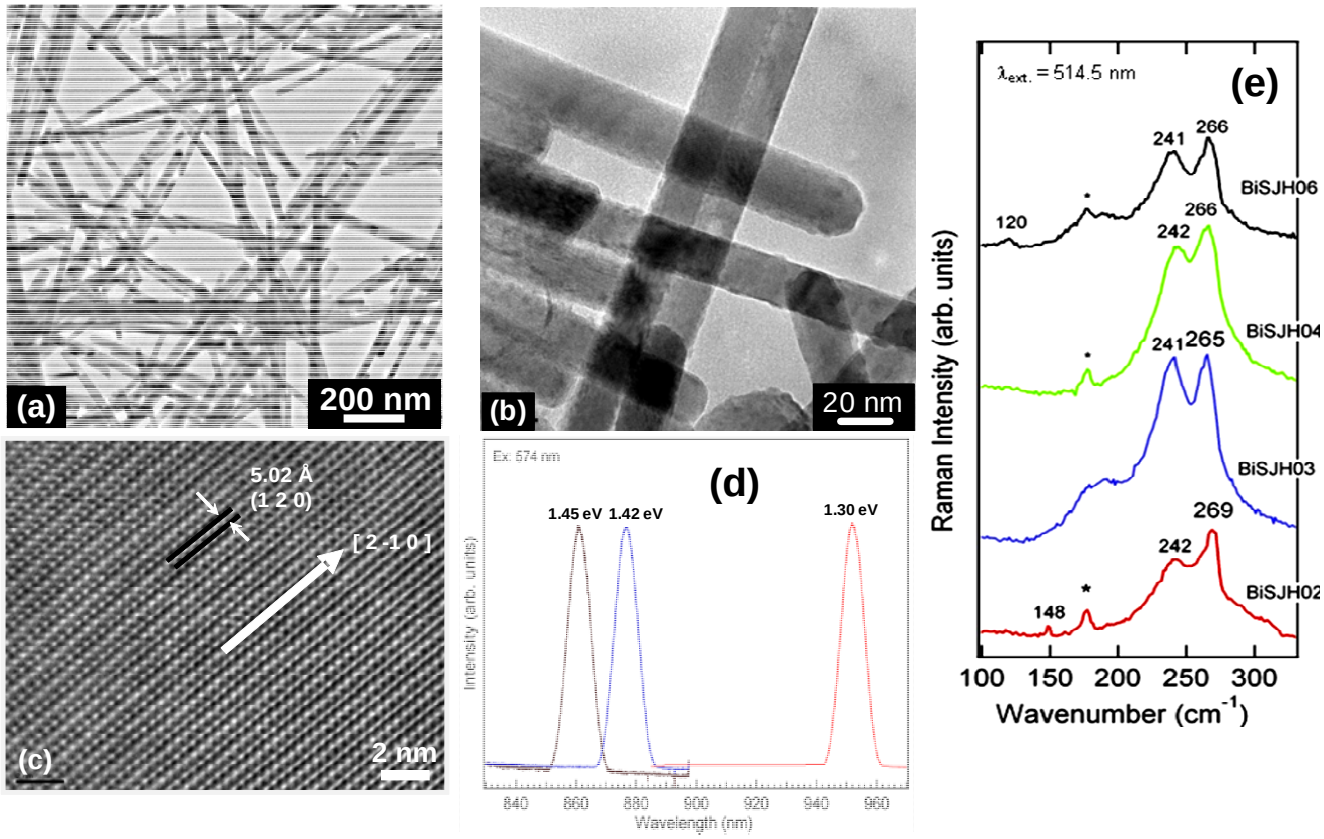

Fig. 14 TEM and HRTEM images of the as-prepared Bi_2S_3 nanorods (a)-(c); Photoluminescence specrum (d) and Raman spectrums (e) of the synthesized nano Bi_2S_3 samples.

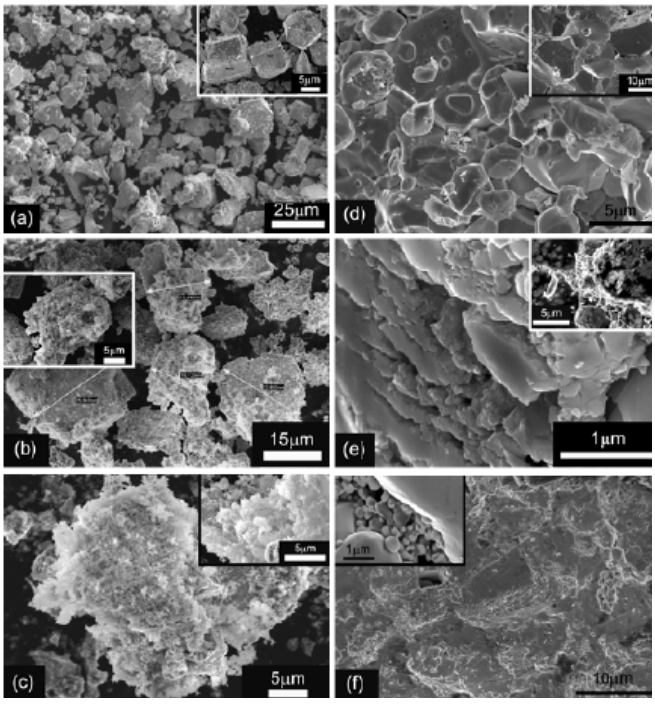

Fig. 15 FESEM images are shown of the as-prepared $CoSb_3$ samples. The nano-particles with typical size of ~ 50 nm plated on the surface of the bulk samples are clearly seen in (b) and (c). (d-f) FESEM images are shown of the bulk-samples that were derived from hot-pressing. In figure (e) and (f), most nanoparticles survived at the inter-grain boundary, in spite of some nano-particles growing slightly under the current hot-pressing conditions.

7 A summary

Table 1 All the nanostructured thermoelectric compounds that have been solution-chemically synthesized by us so far, with their typical morphologies and dimensions

TE compound	Typical morphology and dimension
$CoSb_3$	Spherical granules , 20 - 30 nm
Bi_2Te_3	Spherical granules, 20 - 30 nm; nanowires, nanocapsules, Nanotubes, diameter s of 30 - 50nm, lengths of up to1μm
$Bi_{0.5}Sb_{1.5}Te_3$ $Bi_2Se_{0.3}Te_{2.7}$	Hexagonal chips, length 300 - 400 nm, thickness 10 - 20 nm; Quasi-amorphous irregular particles, 40 - 80 nm
PbTe	Irregular particles, small cubes(~100 nm) and nanorods
PbSe	Flower-like cubic particles (~300 nm), enchased cubes
BiSb	Peanut-like polyhedrals (~100 nm), flower-like structures
Bi_2S_3	Nanorods, ultra-long nanowires (aspect ratio > 5000) and flower like micro-structures
InSb	Irregular diamond-like particles, 30 - 200 nm
TiO_2	Snowballs (500 nm and up), amorphous structures

Conclusions

By means of solution chemical synthesis, many nanostructured state-of-the-art thermoelectric compounds, including Bi_2Te_3 and its based alloys, Bi_2S_3, PbTe & PbSe, BiSb and $CoSb_3$, have been successfully synthesized, with various morphologies of nanoparticles, nano-flakes, nanorods, nanotubes, and so on. These nano thermoelectric materials would be of importance to the current nano and nano-composite thermoelectric research. Some derivative applications like nano-plating and nano coating techniques have also been developed by us from the solution chemical methods, which have been proved useful and promising on nanocomposite fabrication and thermoelectric improvement. Solution chemical approaches are versatile and efficient methods on producing nano materials, and are very favorable to the thermoelectric investigation as well.

Notes and references

The authors thank Mr. J. Reppert and Dr. A. M. Rao at Department of Physics, Clemson University, for their technical assistance on the Raman and Photoluminescence Spectroscopy.

1 A. M. Rao, X. Ji and T. M. Tritt, *MRS Bulletin*, **2006**, *31*, 218.
2 T. Koga, X. Sun, S.B. Cronin, and M.S. Dresselhaus, *Appl. Phys. Lett.*, **1999**, *75*, 2438.
3 X. Sun, Z. Zhang, and M.S. Dresselhaus, *Appl. Phys. Lett.*, **1999**, *74***,** 4005; Y. M. Lin, X.Z. Sun, and M.S. Dresselhaus, *Phys. Rev. B*, **2000**, *62***,** 4610.
4 L. D. Hicks, T. C. Harman, and M. Dresselhaus, *Appl. Phys. Lett.,* **1993**, *63*, 3230; L. D. Hicks and M. S. Dresselhaus, *Phys. Rev. B***,** **1993**, *47*, 12727; W. Kim, J. Zide, A. Gossard, D. Klenov, S. Stemmer, A. Shakouri, and A. Majumdar, *Phys. Rev. Lett.* **2006**, *96*, 045901.
5 T. Nagase, I. Yamauchi, and I. Ohnaka, *J. Alloy. Comp.*, **2000**, *312***,** 295.
6 K. Yanagimoto, K. Majima, S. Sunada, and T. Sawada, *J. Alloy. Comp.*, **2004**. *377***,** 174.
7 J. Yang, T. Aizawa, A. Yamamoto, and T. Ohta, *J. Alloy. Comp.*, **2000**, *309***,** 225.
8 Y. T. Qian, Y. L. Gu, and J. Lu, Chapter in *The chemistry of Nanomaterials: Synthesis, Properties and Applications*, Vol.1. Edited by C. N. R. Rao, A. Müller, A. K. Cheetham. WILEY-VCH Verlag GmbH & Co.KGaA, Wwinheim, **2004**,170.
9 R. Venkatasubramanian, E. Siivola, T. Colpitts, and B. O'Quinn, *Nature*, **2001**, *413*, 597; T. C. Harman, P. J. Taylor, M. P. Walsh, and B. E. LaForge,*Science*, **2002**, *297*, 2229.
10 Y.-M. Lin, O. Rabin, S. B. Cronin, J. Y. Ying, and M. S. Dresselhaus, *Appl. Phys. Lett.*, **2002**, *81*, 2403; M. S. Sander, A. L. Prieto, R. Gronsky, T. Sands, and A. M. Stacy, *Adv. Mater.*, **2002**, *14*, 665; M. Martín-González, A. L. Prieto, R. Gronsky, T. Sands, and A. M. Stacy, *ibid.* **2003**, *15*, 1003.
11 X. B. Zhao, X. H. Ji, Y. H. Zhang, B. H. Lu, *J. Alloys Comp.*, **2004**, *368*, 349.
12 X. Ji, B. Zhang, T. M. Tritt, J. W. Kolis and A. Kumbhar, *J. Elec. Mater.*, **2007**, *36*, 721.
13 X. B. Zhao, X. H. Ji, Y. H. Zhang, G. S. Cao, J. P. Tu, *Appl. Phys. A*, **2005**, *80*, 1567.
14 G. A. Slack and V. G. Tsoukala, *J. Appl. Phys.*, **1994**, *76***,** 1665.
15 T. M. Tritt, *Science*, **1999**. *283***,** 804.
16 R. Tenne, L. Margulis, M. Genut, and G. Hodes, *Nature*, **1992**, *360***,** 444.
17 M. Nath and C.N.R. Rao, *Chem. Commun.*, **2001**: p. 2236.
18 M. Nath and C. N. R. Rao, *Chem. Intern. Ed.*, **2002**, *41***,** 3451.
19 C. N. R. Rao, A. Govindaraj, F.L. Deepak, N.A. Gunari, and M. Nath, *Appl. Phys. Lett.*, **2001**, *78*, 1853.
20 X. C. Jiang, Y. Xie, J. Lu, L.Y. Zhu, W. He, and Y.T. Qian, *Adv. Mater.*, **2001**, *13*, 1278.
21 X. H. Ji, X. B. Zhao, Y. H. Zhang, T. Sun, H. L. Ni and B. H. Lu. *Proceedings of the 23rd International Conference on Thermoelectrics*, ICT2004, Adelaide, Australia.
22 G. A. Slack, New materials and performance limits for thermoelectric cooling, in *CRC Handbook of Thermoelectrics* (D. M. Rowe, ed), **1995**, 407.
23 P. N. Alboni, X. Ji, J. He, N. Gothard, J. Hubbard and T. M. Tritt, *J. Elec. Mater.*, **2007**, ***36***, 711.
24 B. C. Sales, D. Mandrus, R. K. Williams, *Science*, **1996**, *272*, 1325.
25 G. S. Nolas, G. A. Slack, D. T. Morelli, T. M. Tritt, and A. C. Ehrlich. *J. Appl. Phys.*, **1996**, *79*, 4002.
26 Y. I. Ravich, B. A. Efimova and I. A. Smirnov, *Nauka*, Moscow, **1978**.
27 B. Wiley, Y. Sun, J. Chen, H. Cang, Z. Li, X. Li and Y. Xia. *MRS Bulletin*, **2005**, *30*, 356.
28 Y. W. Koh, C. S. Lai, A.Y. Du, E. R. T. Tiekink, and K. P. Loh. *Chem. Mater.* , **2003**, *15*, 4544.
29 X. Ji, J. He, P. Alboni, Z. Su, N. Gothard, B. Zhang, Terry M. Tritt and J. W. Kolis, phys. stat. sol. (RRL), **2007**, *1*, 229.